Supplementary Information

Transient transmembrane secretion of H_2O_2: A mechanism for citral-caused inhibition of aflatoxin production from *Aspergillus flavus*

Jinhan Li,[a,b] Jialin Li,[b] Zhisong Lu,[b*] Yang Liu[a*] and Chang Ming Li [a,b *]

Experimental

Reagents: Dopamine hydrochloride (DA) and 30% H_2O_2 solution were purchased from Aladdin (Shanghai, China). Tris (hydroxymethyl) amiomethane (Tris), catalase, DCFH-DA and glycerin were bought from Sigma–Aldrich (Saint Louis, MO, USA). Citral was purchased from Jiang Xi Xue Song Natural Medicinaloil Co., LTD Other chemicals were of analytical grade and used without further purifications. All solutions used in this study were prepared with deionized (DI) water from Milli-Q-purification system (≥18.2 MΩ cm).

Preparation of PDA microspheres and PDA-Fe_3O_4 nanocomposites: Details of a typical preparation process for the PDA microspheres are described as follows[1]: firstly, 40 mg of DA was dissolved in a mixed solution of ethanol (20 mL) and DI water (15 mL) with magnetic stirring. Then, 10 mL of 3 mg/mL Tris solution was added into the mixture and gently stirred at 25 °C for 24 h. The PDA microspheres were collected by centrifugation with a speed of 14000 rpm for 10 min. After three-time washing with DI water, the final products were dried in vacuum at 40 °C overnight. The PDA-Fe_3O_4 nanocomposites were synthesized based on the previous literature with minor modifications.[2] Briefly, 35 mg PDA microspheres were suspended in 25 mL DI water, followed by addition of 25 mL of 0.79 wt% $Fe_2(SO_4)_3$ solution. After 30 min of ultrasonication at 25 °C and 30 min of ultrasonication at 60 °C, the pH value of the suspension was adjusted to 8.0 with 5 M NaOH. The suspension was sonicated at 60 °C for 30 min, followed by a rest at 60 °C for 20 min. Then pH value of the suspension was changed to 1.0 with 1 M HCl, subsequently adding 50 mL of 0.79 wt% $Fe_2(SO_4)_3$ and 50 mL of 0.59 wt% $FeSO_4$ solutions. The mixture was continuously treated with ultrasonication at 60 °C for another 30 min, and the pH was adjusted to 13.0 again. After a 2-h ultrasonication, the suspension was allowed to rest for 30 min at 60 °C. The Fe_3O_4 NPs-decorated PDA microspheres (PDA-Fe_3O_4 nanocomposite) were harvested by centrifugation, rinsing with DI water and drying in a vacuum oven at 50 °C for 24 h.

Material Characterization: Morphologies of the as-prepared PDA microspheres and PDA-Fe_3O_4 nanocomposites were characterized with SEM (JSM-6510LV, JEOL, Tokyo, Japan). Transmission electron microscopy (TEM) image was obtained using a JEOL-2010 electron microscope operating at 200 kV. Crystal structures of the materials were examined using XRD (MAXima-X 7000, Shimadzu, Japan, 40 kV, 30 mA) with Cu-Kα radiation. FTIR spectra were collected with a FTIR spectrometer (NICOLET 6700, Madison, Wi, USA) in the range of

400–4000 cm^{-1}.

Fabrication of hydrogen peroxide electrochemical sensor: The PDA-Fe_3O_4 nanocomposites based H_2O_2 electrochemical sensors (PDA- Fe_3O_4-Nafion/GCE) were prepared as follows: 10 mg PDA-Fe_3O_4 nanocomposites were dispersed into 2 mL DI water and ultrasonicated for 30 min. 5 μL of the suspension was dropped on a clean glassy carbon electrode (GCE, 3.0 mm in diameter), drying in air. 1 μL of 0.5% Nafion solution was deposited on the modified electrode surface to prevent the leakage of the nanocomposites. For comparison, bare GCE, PDA/GCE and Fe_3O_4-Nafion/GCE were prepared under the identical conditions. Electrochemical measurements were conducted using a CHI660D electrochemical workstation (ChenHua Instruments Co., Ltd., Shanghai, China) with three-electrode system, which includes a bare GCE or modified GCE as the working electrode, a platinum wire as the counter electrode and a Ag/AgCl electrode as the reference electrode. 0.01 M PBS solution (pH 7.4) was applied as supporting electrolyte in all electrochemical tests.

The influence of citral to *Aspergillus flavus*: *A. flavus* GD-6 isolated by our group[3] was used as model fungi in the present study. It was cultured in 250 ml conical flasks containing 100 mL of yeast extract with supplements medium (YES). After 60-hour shaking growth at 30 °C, the mycelia were collected by filtration through two layers of cheesecloth, washing with sterile DI water and PBS solution (0.01M, pH 7.4) successively. The mycelia were suspended in a PBS (0.01M, pH 7.4) solution and treated with 300 ppm citral or glycerin, the electrochemical responses detected by PDA- Fe_3O_4-Nafion/GCE and the level of intracellular ROS analyzed by fluorescence. The morphologies of mycelia were characterized with SEM.

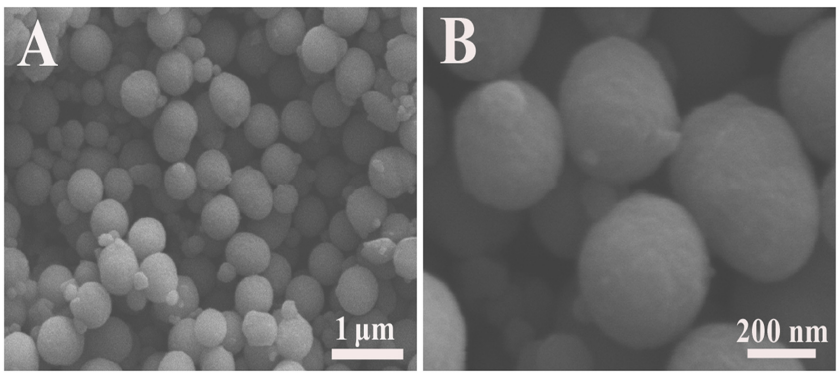

Fig. S1 SEM images of the PDA microspheres

SEM images show that the PDA microspheres have a relative smooth surface and the average size of them is about 250 nm (Fig. S1A and 1B), which is consistent with the findings in Yue's work.[1]

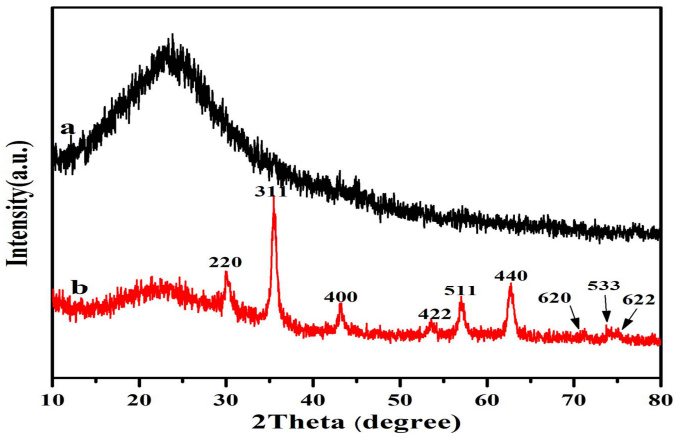

Fig. S2 XRD patterns of PDA microspheres (a) and PDA-Fe_3O_4 nanocomposites (b)

The crystalline phases of the PDA-Fe_3O_4 nanocomposites were analyzed using XRD with PDA microspheres as control (Fig. S2). The broad peak in curve (a) of Fig. S2 suggests the amorphous nature of PDA.[4] As to PDA-Fe_3O_4 nanocomposites, nine well-defined peaks at 30.1°, 35.5°, 43.1°, 53.5°, 57.0°, 62.6°, 71.0°, 74.0°and 75.0° (Fig. S2, curve b) are observed, which can be indexed to the (220), (311), (400), (422), (511), (440), (620), (533) and (622) planes of the cubic Fe_3O_4 ((JCPDS no.65-3107) respectively. The XRD data agrees well with the HRTEM results, proving the existence of the Fe_3O_4 nanocrystallines in the nanocomposites without contamination of Fe_2O_3 NPs.[5]

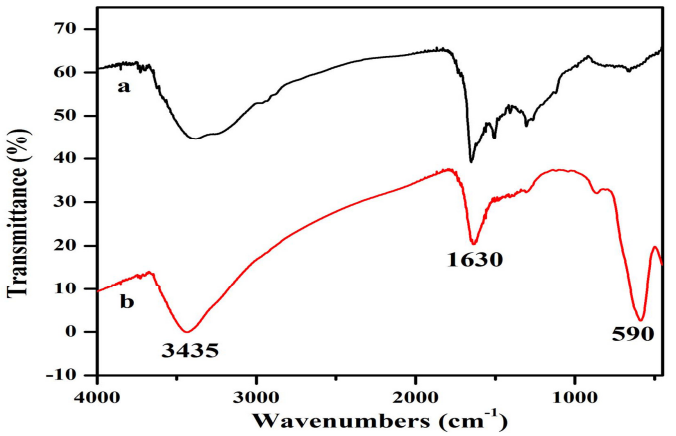

Fig. S3 FTIR of PDA microspheres (a) and PDA-Fe_3O_4 nanocomposites (b)

FTIR was also performed to analyze the surface functional groups of PDA microspheres and PDA-Fe_3O_4 nanocomposites (Fig. S3). The bands at 3435 and 1630 cm^{-1}, which exist in both samples, are ascribed to the aromatic rings and catechol –OH groups of PDA, respectively.[1] A strong peak locates at 590 cm^{-1} only occurs in the FTIR spectrum of PDA-Fe_3O_4 nanocomposites, attributing to the Fe–O stretching of Fe_3O_4.[1] Differently from the peak located at 630 cm^{-1} for γ- Fe_2O_3,[6] the results reveal that the magnetic nanoparticles deposited on the PDA microspheres surface are of a nature of Fe_3O_4. The synthesis of Fe_3O_4 NPs on PDA microspheres has no significant

effects on the band of catechol –OH groups, indicating that the –OH groups are not involved in the Fe_3O_4 NPs formation. The excellent hydrophilicity of the PDA could be maintained in the nanocomposites for the easy access of H_2O_2 molecules in the sensing applications.

Table S1 Comparison of the performance of iron oxide-based electrochemical H_2O_2 sensors

Electrode materials	Sensitivity (μA/mM)	LDR (μM)	LOD (μM)
α- Fe_2O_3–CH[7]	283.6	0.5-15	0.08
Fe_3O_4 /chitosan[8]	9.6	25-5000	7.4
Fe_3O_4[8]	3.6	25-1000	＞7.4
PB- Fe_2O_3[9]	7.27	20–300	7
RGO/ Fe_3O_4[10]	0.0281	100–6000	3.2
α- Fe_2O_3 /rGO[11]	126.9	5.0–4495.0	1.0
(PDDA/Fe_3O_4 NPs)$_5$ multilayer film[12]	-	4.18-800	1.6
PDA-Fe_3O_4	51.06	0.5-12	0.049

Iron oxide-based non-enzymatic electrochemical H_2O_2 sensors that were fabricated in different laboratories have been summarized in Table S1 with respect to the sensitivity, the linear detection range (LDR) and the limit of detection (LOD). In comparison with the reported ones, the PDA-Fe_3O_4 based non-enzymatic electrochemical sensor has a comparable sensitivity and a lower detection limit.

Table S2 The concentration of AFB_1 with different culture time

Time (h)	**AFB_1（ng/mL）**	**ΔAFB_1（ng/mL）**
24	0	-
36	231.25±1.99	231.25±1.99[a]
48	387.48±2.04	156.23±0.45[b]
60	560.36±1.93	172.88±3.97[c]
84	5366.90±8.22	4806.54±6.33[d]
108	8065.58±14.49	2698.68±6.35[e]

1. Q. Yue, M. Wang, Z. Sun, C. Wang, C. Wang, Y. Deng, D. Zhao, Journal of Materials Chemistry B, 2013, 1(44), 6085-6093.
2. W. Zhao, L. Zhu, Y. Lu, L. Zhang, R.H. Schuster, W. Wang, Synthetic Metals, 2013, 169, 59-63.
3. C. Zhang, F. Xing, J.N. Selvaraj, Q. Yang, L. Zhou, Y. Zhao, Y. Liu, Biochemical Systematics and

Ecology, 2013, 50, 147-153.

4. (a) F.Wang, R. Han, G. Liu, H. Chen, T. Ren, H. Yang, Y. Wen, Journal of Electroanalytical Chemistry, 2013, 706, 102-107; (b) M. Zhang, X. He, Y. Zhang, Journal of Materials Chemistry, 2010, 20, 10696-10704.
5. W. Zhang, X. Wu, J. Hu, Y. Guo, L. Wan, Advanced Functional Materials, 2008, 18, 3941-3946.
6. Y. Xiong, J. Ye, X. Gu, Q. Chen, Journal of Physical Chemistry C, 2007, 111, 6998-7003.
7. L. Zhang, Y. Ni, X. Wang, G. Zhao, Talanta, 2010, 82(1), 196-201.
8. M.S. Lin, H.J. Leu, Electroanalysis, 2005, 17(22), 2068-2073.
9. A.K. Dutta, S.K. Maji, D.N. Srivastava, A. Mondal, P. Biswas, P. Paul, B. Adhikary, Journal of Molecular Catalysis A-Chemical, 2012, 360, 71-77.
10. Y. Ye, T. Kong, X. Yu, Y. Wu, K. Zhang, X. Wang, Talanta, 2012, 89, 417-421.
11. M. Wang, T. Shen, M. Wang, D. Zhang, Z. Tong, J. Chen, Sensors and Actuators B-Chemical, 2014, 190, 645-650.
12. L. Zhang, Y. Zhai, N. Gao, D. Wen, S. Dong, Electrochemistry Communications, 2008, 10(10), 1524-1526.